Physica C 518 (2015) 81–84

Contents lists available at ScienceDirect

Physica C

journal homepage: www.elsevier.com/locate/physc

Layer number dependence of flux avalanches in superconducting shifted strip array

A. Mine [a], Y. Tsuchiya [a], S. Miyano [a], S. Pyon [a], T. Tamegai [a,*], S. Nagasawa [b], M. Hidaka [b]

[a] Department of Applied Physics, The University of Tokyo, 7-3-1 Hongo, Bunkyo-ku, Tokyo 113-8656, Japan
[b] National Institute of Advanced Industrial Science and Technology (AIST), Tsukuba, Ibaraki 305-8568, Japan

ARTICLE INFO

Article history:
Received 7 February 2015
Received in revised form 11 March 2015
Accepted 25 March 2015
Available online 12 April 2015

Keywords:
Nanostructured superconductor
Flux penetration
Flux avalanches
Magneto-optical imaging

ABSTRACT

We have fabricated multi-layer superconducting shifted strip arrays (SSAs) of Nb up to 4 layers and systematically studied the vortex penetrations into these structures. We observed the vortex penetration as a function of the number of layers and the ratio of overlap between neighboring layers by using magneto-optical (MO) imaging. In the case of 2- and 3-layer SSAs, spot-like avalanches occur when the overlap is small, while linear avalanches occur when the overlap is large, consistent with our previous reports. In the 4-layer SSAs, the smallest limit of the overlap between the neighboring layers for the linear avalanche is lower. Flux penetrations parallel to the strip which were observed in the 3-layer SSA were also observed in the 4-layer SSAs with smaller ratio of overlap. Larger demagnetization effects in the middle two layers in 4-layer SSA help to make avalanches larger and more extended.

1. Introduction

Remarkable developments of microlithography technology to fabricate submicron-sized objects have been applied to the fabrication of complicated superconducting structures called "nanostructured superconductors". Nanostructured superconductors have various kinds of applications, such as single flux quanta (SFQ) devices [1], which can operate much faster than CMOS devices with less energy, and single photon detector (SPD) [2]. On the other hand, magnetic cloaking metamaterial [3–5], which can shield the external magnetic field without disturbing the external magnetic flux distribution can be constructed using nanostructured superconductors with anisotropic permeability [6,7]. Several kinds of superconducting metamaterials have been proposed consisting of relatively simple building blocks such as squares and long strips. Anisotropic permeability has been experimentally demonstrated and calculated for a superconducting metamaterial consisting of many sheets of square array of square Pb films [8,9]. Theoretically, stacks of strips in different arrangements are calculated [10]. According to these calculations, both rectangular array, which is a strip array both along the layer and perpendicular to it, and hexagonal array, which is a strip array stacked many layers shifting positions by a half period, have anisotropic permeability. A hexagonal array can produce larger anisotropy in the permeability than a rectangular array due to larger overlaps between the neighboring layers. However, the same characteristic can lead to the flux avalanche due to thermomagnetic instability [11].

We have already reported that peculiar flux avalanches occur in a shifted strip arrays (SSAs) of Nb [12–15], which are hexagonal arrays with only two or three layers. In SSAs, various forms of flux avalanches occur even though the width of each single strip is much narrower than the threshold width for such an instability [11]. In particular, when the overlap ratio w/a (w: width, a: period of the strips) is large, since the heat produced by avalanche causes another avalanche in the other layer one after another, linear avalanches perpendicular to the strips were observed. In 3-layer SSA, flux penetration along strips can be observed. Since 2- and 3-layer SSA have no or only one middle layer, the form of avalanche in these SSA can be different from those in a hexagonal array. In this paper, we extend these observations using magneto-optical (MO) imaging to SSAs with layer numbers up to four to infer the form of avalanche in a hexagonal array.

2. Experiments

We have fabricated three-dimensional nanostructured superconductors of Nb (T_c = 9.2 K) with insulating SiO_2 on a Si substrate. The fabrications of the device including the caldera planarization [16] were done in the Clean Room for Analog–digital superconductiVITY (CRAVITY) in The National Institute of

* Corresponding author. Tel.: +81 3 5841 6846; fax: +81 3 5841 8886.
E-mail address: tamegai@ap.t.u-tokyo.ac.jp (T. Tamegai).

http://dx.doi.org/10.1016/j.physc.2015.03.012
0921-4534/

Advanced Industrial Science and Technology (AIST). As shown in Fig. 1(b), narrow strips (w = 20 μm) of Nb along y-axis are periodically arranged along x-axis with a period "a" in each layer. Such strip arrays are stacked on top of each other by shifting a half period with SiO_2 layers between them as shown in Fig. 1(a). We call these structures shifted strip arrays (SSAs). Strip arrays up to four layers are stacked in the SSAs to observe the different forms of flux penetrations and avalanches. The width of the strip, w, is fixed to 20 μm, with its length (l) and thickness (d_s) 300 μm and 300 nm, respectively. Strips in each layer are separated by SiO_2 with a thickness of d_i = 300 nm. The overlap ratio w/a and number of strips in each layer n in the studied SSAs are as follows; $(w/a, n)$ = (60%, 11), (75%, 12), (90%, 12).

Flux penetrations into SSAs are observed by using the magneto-optical (MO) imaging, where local field induced Faraday rotation of linearly polarized light in the indicator garnet film is detected through a polarizer. The MO image was captured using a polarizing microscope (Olympus BX30MF) with 550 nm wavelength filter and a cooled CCD-camera with 12 bit resolution (ORCA-ER Hamamatsu). The SSA samples are cooled by a He-flow cryostat (Microstat HighRes II, Oxford Instruments). We calibrate our indicator garnet film at 10 K, which is higher than the T_c of Nb. After zero-field cooling (ZFC) to 5 K, the external field perpendicular to the plane of the SSA is increased in a step-wise manner. MO images are constructed by subtracting the integrated background image at zero field from the image at a certain magnetic field [17]. An in-plane field is also applied to suppress the appearance of in-plane magnetic domains in the garnet.

3. Results and discussion

Examples of MO image of flux penetrations into SSAs with different numbers of layers and overlap ratios at 5 K are shown in Fig. 2. We start with the comparison between spot-like avalanches into the 2- and 3-layer SSAs in the present experiments with w = 20 μm and those in our previous reports with w = 8 μm [12,13]. Both in our previous reports and the present study, spot-like avalanches occur when the overlap ratio w/a is small, while linear avalanches occur when the overlap ratio w/a is large. However, spot-like avalanches occurred in only one strip in our previous reports for w/a = 73% (w = 8 μm, a = 11 μm) [12,13], while they occur across more than one strip for w/a = 75% in the present study. The spot-like avalanches similar to the previous report with w/a = 73% occurs in the case with w/a = 60% in this study. Fig. 3(a)–(f) describes the difference between the two types of spot-like avalanches in the present experiments. For w/a = 60%, a spot-like avalanche starts from the top layer (Fig. 3(a)), and it only triggers another small avalanche in the bottom layer (Fig. 3(b)). In this case, the MO image seen from the top looks like Fig. 3(c). By contrast, spot-like avalanche starts from the top layer for w/a = 75% triggers two avalanches in the bottom layer (Fig. 3(d)) because of the larger avalanche than that in the SSA with w/a = 60% due to the larger demagnetization effect. One of the two triggers the third one in the top layer (Fig. 3(e)). In this case, the MO image seen from the top looks like Fig. 3(f). In the experimental MO images, the penetrations into the second top layer are expanded by the shielding of the top layer.

In the 3-layer SSA, the previous result for spot-like avalanches is similar to the result for w/a = 60% rather than 75% in the present experiment. It can be explained by the same way as in the 2-layer SSA. Flux penetrations in the 3-layer SSA with w/a = 75% is explained as shown in Fig. 3. In this model, flux penetrations along y-axis can occur only after the avalanche across the strip divides the strip as shown in Fig. 4(a). In the 3-layer SSA with w/a = 75%, such avalanches across the strip occurs and flux can penetrate along y-axis as shown in Fig. 4(c).

Now we compare the flux penetration into the 4-layer SSAs and those into the 2- or 3-layer SSAs in the present experiments. When w/a is 60%, spot-like avalanches occur in 4-layer SSA, which are similar to 2-layer and 3-layer SSAs. Differences in the demagnetization effect between layers are described in Fig. 5(a)–(c). In the 3-layer SSA, the avalanches in the middle layer are larger than those on the top and bottom layers. This observation supports the claim that the first avalanche occurs in the middle layer with a large demagnetization effect due to the presence of Nb layers above and below the layer. The same tendency can be observed in the 4-layer SSA. Namely, avalanches in the second top layer is little larger than those in the top layer. In the same way, the avalanches in the top and bottom layers are the same size as those in the 2-layer SSA, which have two layers with the same demagnetization effect.

When w/a is 75%, linear avalanches occur in the 4-layer SSA, while spot-like avalanches occur in 2-layer and 3-layer SSAs. First, we compare the width of avalanches along y-axis in the 4- and 2-layer SSAs. The widths of the avalanches in the 4- and 2-layer SSAs are not so different. However, the width of the widest part, where linear avalanche started, in the 4-layer SSA is clearly larger than that in the 2-layer SSA. The wider the avalanche is, the larger the heat generated by avalanche should be. Therefore the first avalanche in 4-layer SSA generates larger heat than those in 2-layer SSA. Large demagnetization effect in 4-layer SSA will make the first avalanche larger than 2-layer SSA. Therefore, linear avalanches are more easily triggered in the 4-layer SSAs than in the 2-layer SSAs.

Next, we discuss the possible reason for the absence of clear linear avalanches in the 3-layer SSA. The middle layer has a larger demagnetization effect than others as we noted above (Fig. 5(b)). When the first avalanche occurs in the middle layer and generates heat, it can cause the avalanche in the top layer. However, because of the smaller demagnetization effect in the top layer, the heat generated by the avalanche in the top layer is not sufficient to cause another avalanche in the middle layer. By contrast, in the case of 4-layer SSA, the middle two layers have the same demagnetization effect (Fig. 5(c)). In this case, the first avalanche starts from the second top layer due to the large heat transfer of Si substrate than that

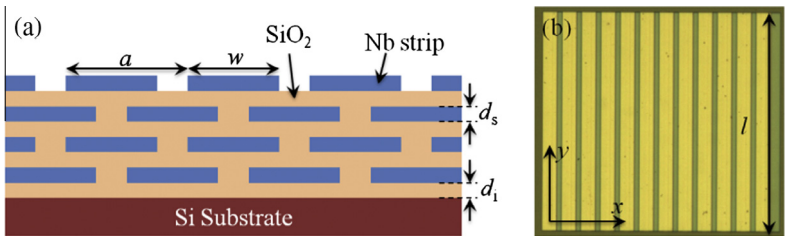

Fig. 1. (a) Schematic cross section of the 4-layer SSA perpendicular to y-axis. (b) An optical image of 4-layer SSA (w/a = 75%). The top layers of each SSA do not contain SiO_2. The letters a, w, d, and l denote the lattice constant, strip width, layer thickness, and strip length, respectively.